ELSEVIER

Polymer 43 (2002) 1887–1895

polymer

www.elsevier.com/locate/polymer

Crystal melting and its kinetics on poly(ethylene oxide) by in situ atomic force microscopy

L.G.M. Beekmans[a], D.W. van der Meer[a,b], G.J. Vancso[a,b,*]

[a]*Department of Materials Science and Technology of Polymers and MESA+ Research Institute, University of Twente, AE Enschede, The Netherlands*
[b]*Dutch Polymer Institute, P.O. Box 217, 7500 AE Enschede, The Netherlands*

Accepted 12 November 2001

Abstract

The process of melting in poly(ethylene oxide) (PEO) is followed in real-time at elevated temperatures by atomic force microscopy (AFM) using a simple hot stage apparatus. AFM imaging of the morphology above the onset of melting revealed the dynamics of a complex melting process. The observed melting behavior of PEO is associated with the existence of separate dominant and subsidiary morphological entities. The morphological observations revealed that the melting process is not explained by a mechanism of crystal reorganization (melting–recrystallization–remelting or crystal thickening. The kinetic data shows that the crystal dimensions decrease proportional to time indicating a nucleation controlled melting process. The crystals melt instantaneously on heating and reveal a spread in the rates of melting of the radial {120} faces. This variation in rate of retrogression of the crystals is assumed to be related to a lamellar thickness distribution of the melt grown crystals. © 2002 Published by Elsevier Science Ltd.

Keywords: Melting kinetics; Poly(ethylene oxide); In situ atomic force microscopy

1. Introduction

The melting and crystallization behavior of isothermally crystallized polymers have been a subject of continued interest for many years [1]. The thermodynamics of the melting process, usually studied by differential scanning calorimetry (DSC), manifests itself as a broad melting endotherm [2–7]. Different approaches have been postulated to explain the melting process. One of the earliest, and most generally accepted, comprises a recrystallization mechanism, in which it is proposed that the original crystals structurally reorganize into more perfect or thicker crystalline structures during melting, i.e. into crystals of higher melting temperatures [6,7]. This model is experimentally supported by the shift of the peak of the melting endotherm to higher temperatures at slower DSC scanning rates. The second model describes the melting process as morphologically the reverse of the isothermal crystallization process [2,4,8]. During isothermal crystallization, the crystal growth involves initially the formation of dominant lamellae and in a subsequent step by the development of subsidiary lamellae which fill in the space between the former crystals [8,9]. There is a concomitant segregation, since the dominant lamellae will contain the longest molecules while the subsidiary ones contain the material initially rejected. This fractionation results in a distribution of crystal thickness and is supposed to contribute to the broadening of the melting endotherm. Both hypotheses have received considerable support by results obtained using several experimental techniques [2,4,5]. One of the first successes of the modulated DSC (MDSC) technique has been the ability to resolve the thermal contribution that results from the reorganization process, such as in the case of poly(ethylene oxide) (PEO) [10].

Despite the general interest in polymer melting, relatively little attention has been directed towards studies of the melting kinetics of polymer crystals in the past 25 years. It is anticipated that any process that occurs during melting should manifest its effect clearly in the kinetics. Melting rates have been reported only in the case of large single crystals of low molar mass PEOs which permit analysis by optical microscopy (LM) [11–13]. Kovacs et al. found that the crystal dimensions decreased at a rate, which is proportional to the time of melting. From these observations, it was concluded that a nucleation process must be the rate-controlling step in the melting of the single crystals.

* Corresponding author. Address: Department of Materials Science and Technology of Polymers and MESA+ Research Institute, University of Twente, P.O. Box 217, 7500 AE Enschede, The Netherlands. Tel.: +31-53-489-2974; fax: +31-53-489-3823.

E-mail address: g.j.vancso@ct.utwente.nl (G.J. Vancso).

0032-3861/02/$ - see front matter © 2002 Published by Elsevier Science Ltd.
PII: S0032-3861(01)00748-0

Previous studies [11–13] proposed a correlation between crystallization and melting, suggesting that both processes are nucleation controlled. However, these studies do not provide insight into the mechanism by which this process is transmitted to the higher structural levels of the spherulite. When observed by LM, melt-crystallizing spherulites indeed grow at a linear rate, resulting in locally birefringent structures. On the other hand, melting of the spherulitic structure is accompanied by a uniform decrease of the depolarized light intensity. The crystal aggregates do not melt radially inward by decreasing the radius at a rate which is proportional to the time. Therefore, a new study was initiated in search of the contributing factors that could describe the mechanism that leads to the melting of polymer spherulitic aggregates. Accordingly, this paper communicates the results of an investigation of the melt kinetics on a lamellar crystal level accompanied by in situ morphological observations.

Electron microscopy (EM) has afforded remarkable insight into the lamellar structure of semi-crystalline polymers. However, this technique cannot be used to examine the melting and crystallization process as they occur, i.e. real-time. The ability of AFM to follow real-time dynamics of processes, albeit with some limitations in speed, is now well established. The morphological changes and crystal growth kinetics at the lamellar crystal level were reported [14–22]. However, melting in contrast to crystallization is a fast process under low degrees of superheating. Therefore, AFM melting examinations, up to now focused on feasibility studies [16–18,22].

For this study PEO was chosen because its melting behavior has been studied in detail on a lamellar level in great detail by LM [11–13]. The low temperatures at which melting and crystallization occur ($T_m^0 = 76$ °C) [23] makes PEO an optimal subject for the study of the melting process in real-time, by AFM. The present work is unique in the sense that it reports direct observation of PEO isothermal melting kinetics at a lamellar crystal level.

2. Experimental

PEO was obtained from Aldrich (weight average molar mass 2,000,000 g/mol) and was precipitated from chloroform into methanol prior to use. The precipitate was first dried in air and then dried in vacuum for 1 day. Samples were prepared for AFM melting studies by first pressing the polymer between two glass cover-slides in a thermally controlled (Mettler FP80) microscope hotstage (Mettler FP82) at 90 °C, where the polymer was melted for 5 min and then cooled to the temperature of crystallization within approximately 1 min. The glass cover-slides were then taken out from the hotstage and the top cover-slide was removed, leaving a polymer film of estimated thickness of 30–80 μm.

AFM experiments were performed in air using a NanoScope III setup (Digital Instruments). The instrument was equipped with a J-scanner (maximum scan size 100 μm^2). Commercially available Si_3N_4-cantilevers were used with force constants of 0.38 N/m as stated by the manufacturer. Measurements were carried out in contact mode, always using the smallest possible set-point value to minimize interaction forces between the tip and sample, unless otherwise reported. Height and deflection images were acquired simultaneously. The AFM heating stage used in the AFM was a modified set-up of a previously published design [24]. A small k-type disk thermocouple was used to measure temperature, which was also calibrated using compounds of known melting points (benzophenone, and chlorobenzophenone).

A Perkin–Elmer calorimeter Pyris 1, DSC was calibrated using gallium and indium before use. All DSC scans were recorded at 10 °C/min. The sample chamber was kept under a constant flux of nitrogen. When crystallization was complete, the samples were quickly cooled to 30 °C and the melting thermograms were recorded. For the measurement of thermal stability a Perkin–Elmer thermogravimetric analyzer, TGA-7 was used. The sample chamber in these experiments remained under a constant flux of air. Isothermal melting experiments were performed on samples isothermally crystallized at 55 °C by heating the samples at 10 °C/min to the selected temperature of 69 °C. The sample weights were recorded for 780 min at this holding temperature. After this the samples were quickly cooled to 30 °C. Gel permeation chromatography (GPC) measurements were carried out in $CHCl_3$ using microstyragel columns HR 4, HR 5, HR 2 and, HR 1 (Waters) equipped with a differential refractometer (Walter model 410) detection system.

Small angle X-ray scattering (SAXS) patterns were obtained at beamline ID2 at the European synchrotron radiation facility (ESRF), Grenoble, France with a monochromatic wavelength of 0.995 Å. The sample to detector distance was 10 m. The diffraction patterns were recorded on a two-dimensional Princeton CCD detector. Using the FIT2D program, the 2D patterns were transformed into one-dimensional patterns by performing integration along the azimuthal angle. Lorentz correction was made by multiplying the scattering intensity with the scattering vector (q^2).

3. Results and discussion

3.1. General observations for PEO melting

The DSC melting traces of isothermally crystallized PEO samples are shown in Fig. 1. The melting endotherm for the sample isothermally crystallized at 45 °C displays a single melting region and a broad melting range exhibiting a width of approximately 15 °C. For comparison the melting behavior of the PEO crystals grown at lower degree of undercooling is also measured by DSC. Fig. 1 contains

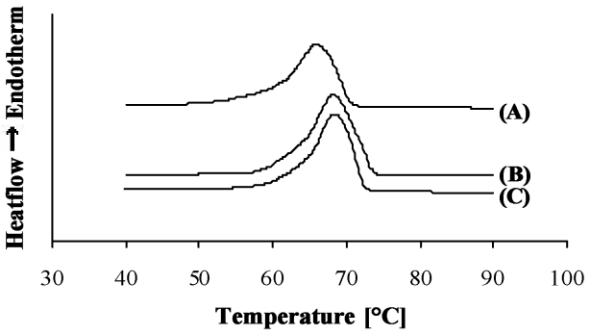

Fig. 1. (A–C) DSC melting thermograms of (A) a PEO sample isothermally crystallized at 45 °C for 4 h, (B) at 55 °C for 4 days, (C) at 55 °C for 4 h, all quenched cooled to 30 °C and subsequently heated. All samples were heated at a rate of 10 °C/min.

corresponding representative DSC heating traces of PEO samples isothermally crystallized at 55 °C for 4 h and 4 days, respectively. Both melting scans display single, broad melting endotherms. The melting peak has not shifted due to the prolonged annealing at the temperature of crystallization which seems to indicate that the lamellar crystals have not thickened or reorganized by rejection of crystal defects. The melting peak of the crystal grown at lower degree of undercooling shifted to higher temperature by approximately 3 °C. Thus as expected the crystals in these structures exhibit a higher thermal/thermodynamic stability as compared to the crystals grown at 45 °C. Similar calorimetric results for PEO were published by Cheng and Wunderlich [3].

AFM feasibility studies of PEO melting indicated that the process of melting was akin of thermal etching [16,17]. An example of the melting behavior in PEO is shown in Fig. 2. The image in Fig. 2(A) was acquired at room temperature

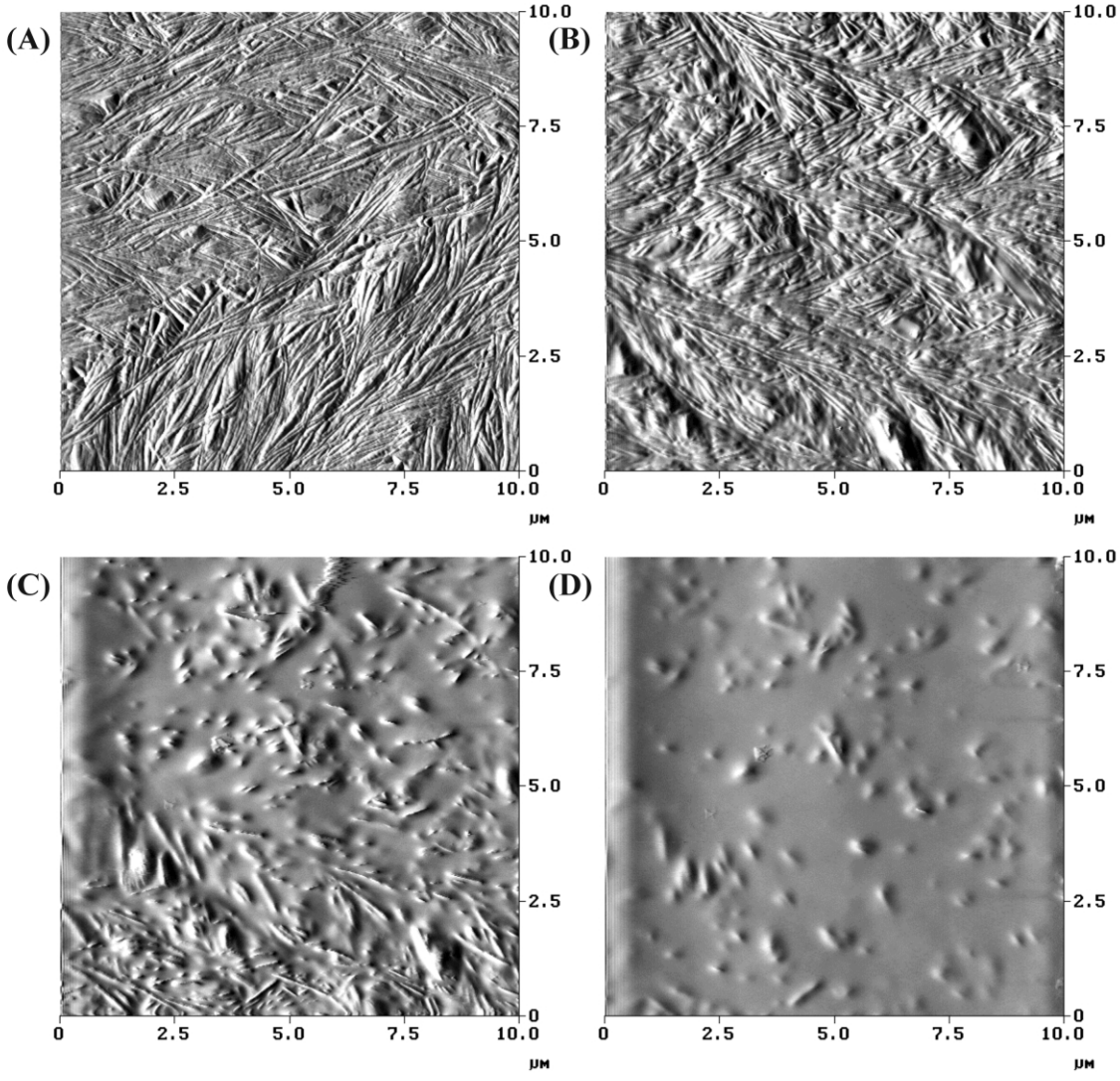

Fig. 2. (A–D) AFM deflection images of a PEO spherulite grown at 45 °C at (A) room temperature, (B) 67 °C and (C,D) 70 °C. The image in (B) was acquired after 32 min at 67 °C. The successive images in (C), and (D) were acquired after 8, 11 min, respectively, at 70 °C.

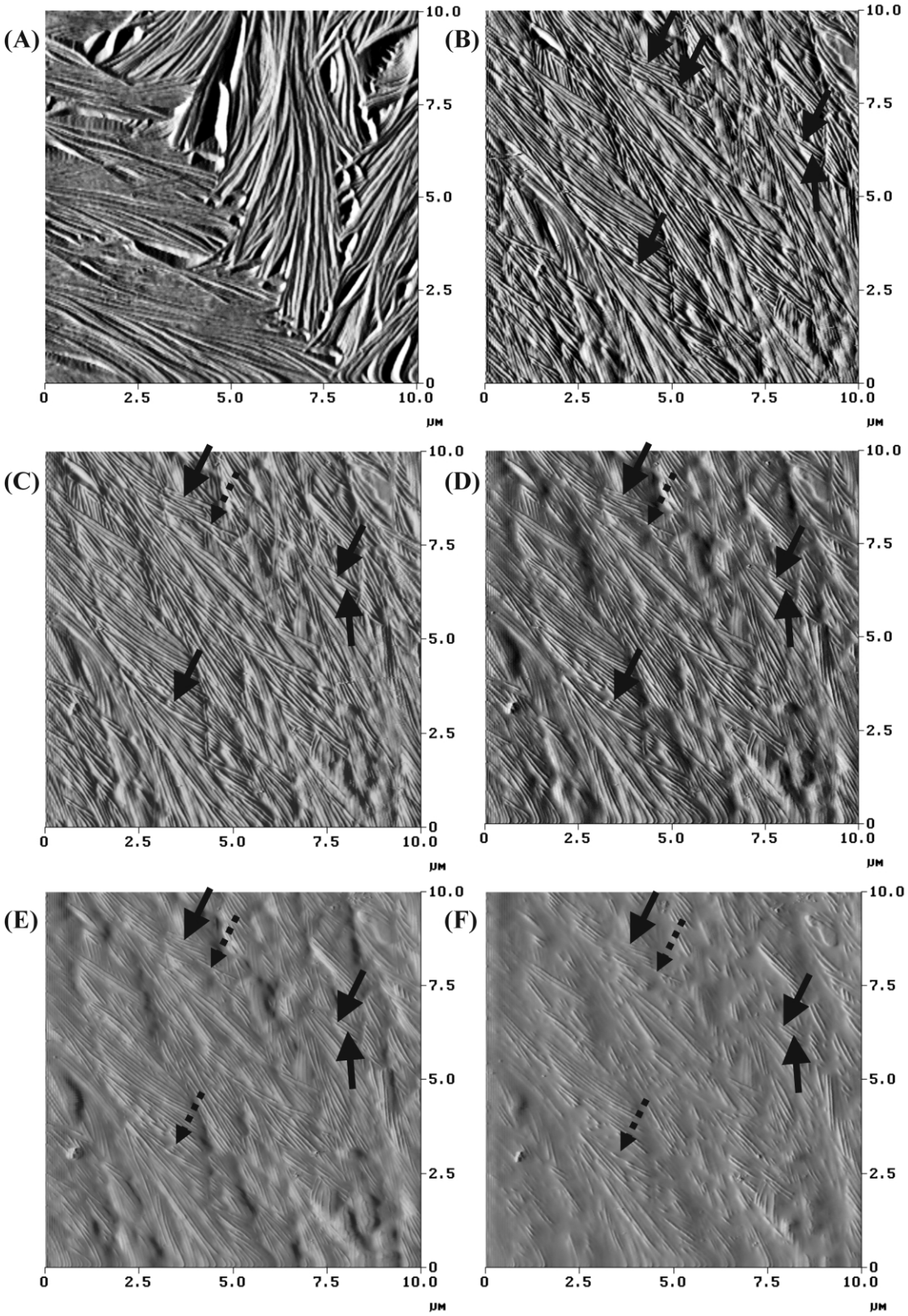

Fig. 3. (A–F) AFM deflection images of a PEO spherulite grown at 55 °C for 4 days, obtained at (A) room temperature and (B–F) 69 °C. The successive images in (C), (D), (E) and (F) correspond to elapsed times of 15, 34, 53 and 95 min, respectively, with respect to the image in (B).

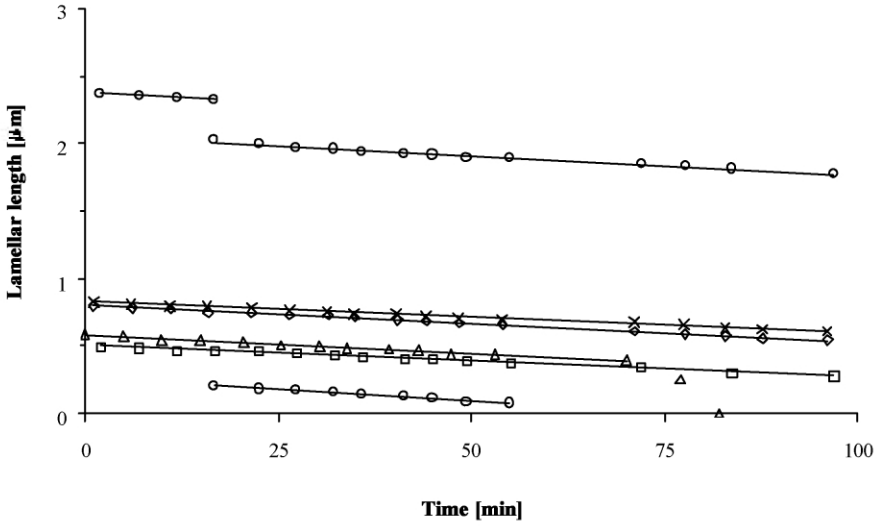

Fig. 4. Lamellar crystal melting at 69 °C. Length versus time data for different individual PEO lamellar crystals as indicated by the arrows in Fig. 3(B)–(F).

and it reveals the complex, ordered lamellar crystal morphology within the PEO spherulites isothermally crystallized at 45 °C. The image in Fig. 2(B) shows a similar section of another spherulite acquired at the elevated temperature of 67 °C. This temperature is near to the peak melting temperature of PEO as observed by DSC. It can be seen in the image that the melting process has started prior to capturing the image. Fig. 2(C) and (D) shows images of approximately the same region as in Fig. 2(B), but now acquired at 70 °C. This temperature is near the end of melting range as seen in the DSC melting scan in Fig. 1.

The fast melting rates at 70 °C result in a non-uniform melting process on the time scale of the image. AFM imaging corresponds to a scan rather than a 'snapshot'. In Fig. 2(C), the scan direction was from bottom to top, hence melting has advanced further at the top of the image. The bottom part was in fact acquired approximately 3 min before the upper part. It can be seen that the fast melting kinetics of PEO results in non-uniform melting on the time scale of the image.

3.2. Study of PEO melting kinetics

In view of crystal melting kinetics, our examination concentrated on PEO crystals that are grown at a lower degree of undercooling. This approach is chosen because PEO crystals grown at higher temperatures show a lower degree of morphological complexity as compared to the crystals grown at a higher degree of undercooling. In the terminology of Keith and Padden [25] the morphology in Fig. 2(A) shows a finer detailed lamellar crystal texture as compared to the morphology obtained by isothermal crystallization at 55 °C (Fig. 3(A)). Fig. 3(A) shows the impingement of two separate spherulitic aggregates which are initially grown at 55 °C and annealed for 4 days at the same temperature. The image is acquired at room temperature and shows the lamellar crystal arrangement within the crystal aggregates. It is clearly visible that the crystals exhibit slightly different projections in the two separate spherulitic structures. The lamellar crystals which make up the entity on the right hand side appear to be closer to flat-on.

In Fig. 3(B) a section of a spherulite can be seen after raising the temperature to 69 °C. This temperature of the isothermal AFM melting experiment was located near the maximum of the endothermic DSC peak, i.e. partial melting of the PEO sample is anticipated. The successive images of Fig. 3 allow one to have an insight into the melting process by estimating the melting kinetics on a lamellar crystal scale. The process of melting was found to be slow and uniform on the time scale of the images and lasted for many hours.

The length of the lamellar crystals at 69 °C was measured as a function of time. The results are shown in Fig. 4 for several representative PEO crystals. The melting data shown corresponds to the crystals indicated by the arrows in Fig. 3(B)–(F). The pixel size resolution error for the length measurement in the series of images of Fig. 3 is roughly equal to the size of the data points.[1] A linear fit of the length versus time data resulted in melting rate values with a 99% confidence interval. It can be seen from the melting data that the lamellar crystals melt at a constant rate which is in agreement with the results as reported by

[1] It is important to point out that several effects can affect lamellar thickness determination by AFM. An overestimate of the lamellar thickness by measurement of the edge-on seen crystals is to be expected because of the pixel size resolution of the images (~20 nm), the broadening effect of the tip and crystal orientation. First, the error introduced by the tip size (~20 nm, tip convolution) is decreased by measuring lamellar thickness at half-maximum in the simultaneously recorded height images [19]. Second, if the crystals experience a distinct angle between axis and the surface the measured lamellar thickness will be an overestimate of its actual thickness.

Kovacs and co-workers [11]. Constant linear melting rates were reported by these authors for perfect once-folded and extended chain crystals of low molecular weight PEO fractions suggesting that the melting process is nucleation controlled.

The linear rate of melting indicates that a nucleation-controlled process occurring at the melting front is the rate-controlling step within the spherulitic structures. No melting seems to occur on the fold surfaces of the lamellae except for presumably less perfect crystal sites. Compared to the melting of the low molar mass PEO crystals [11–13] the melting process of a multi-folded crystal consisting of long macromolecules above the entanglement limit as studied here, seems not being influenced by restriction of the chain. These restrictions can include for example, incorporation in other crystals or entanglements in the melt, or folding back to the interior of the same crystal. Therefore, the melting of a polymer chain is constrained to stems adsorbed to the melting front and should start at the fold at the edge of the crystal, working its way down the lateral surface.

The melting rates of individual PEO crystals are shown in the graph of Fig. 5. It shows the kinetic data for the crystals for which the melting rate could be accurately measured. It appears that there is a spread in the rate of retrogression of the individual crystals in the multi-layered spherulitic morphology. It is important to note that the crystallographic continuity in a spherulitic crystal from center to its edge suggests that the lamellar crystals as observed possess similar growth faces [26]. Generally, it is assumed that the differences in melting temperatures of polymer crystals arise from differences in crystal thickness or from different folded surface free energies for the sectors [27]. Based on the crystallographic continuity, we can rule out the effects of differences in fold surface arrangement between sectors. Hence, the difference in thermal stability of the crystals therefore should depend on crystal thickness.

The radial lattice continuity in the spherulite implies that the lamellar crystals are bounded by most likely the radial {120} faces in the view directions of the deflection images [23]. The crystals are presumably aligned with their crystallographic *b*-axis in the plane of view. The differences in melting rates for the {120} faces between individual lamellar crystals is assumed to be a reflection of the variation of their thermodynamic stability (different T_ms). The natural deduction is therefore, that the crystal melting rate difference is caused by different thicknesses of the lamellar crystals. Similar observations have been reported by Kovacs and co-worker based on a LM study of large lamellar PEO bilayer crystals [13].

It has been suggested that segregation is the cause for this thermal difference of the lamellar crystals [8,9]. The longer chains tend to be located in the first forming dominant lamellae of higher melting point. However, segregation of the polymer chains is an effect initiated during the growth of the crystals. It should therefore be present during the crystallization process. Indeed, the kinetic study of large crystal aggregates at a lamellar crystal level led the authors to conclude that the individual crystals at the spherulitic growth front posses a spread in rate of advancement [15,16].

To further understand the spread in melting rates, our efforts concentrated on quantitative measurements of the lamellar crystal thickness by AFM.[1] Values ranging from 60 to 120 nm were estimated from the simultaneously collected height image of Fig. 3(A) for the crystals initially grown at 55 °C. It has been reported that the individual PEO spherulitic crystals nucleate at various depths below the surface and orient randomly [28]. One of the reasons of the broad range of thickness values is associated with the different lamellar orientation in the two separate spherulitic entities.

For comparison, the long period was also measured by SAXS. SAXS data was used to estimate the lamellar thickness. Fig. 6 shows the SAXS data for the PEO samples crystallized at 55 °C for 4 h and 4 days. A scattering peak with a long period of 47 nm was clearly observed for PEO samples isothermally crystallized independent of the total time of crystallization. The crystallinity of this PEO sample was determined from the enthalpy of fusion measured with DSC and approaches a value of 75% [3]. A value of 35 nm was estimated for the lamellar crystals isothermally grown at temperature of 55 °C using the average volume fraction of

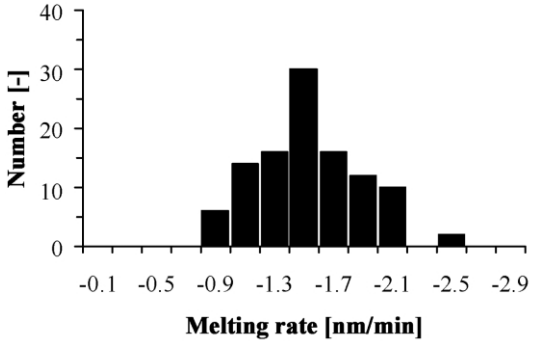

Fig. 5. Lamellar crystal melting rates as measured at 69 °C of PEO isothermally crystallized at 55 °C.

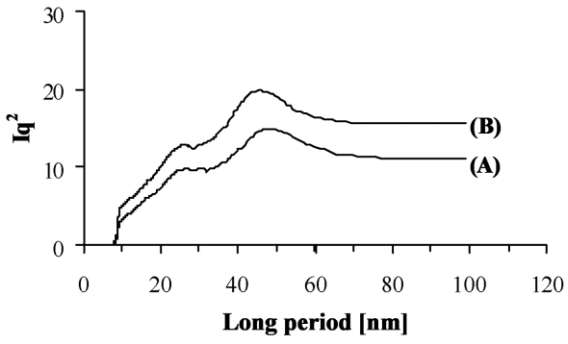

Fig. 6. (A,B) Synchrotron SAXS data for PEO isothermal crystallized at 55 °C for 4 h and 4 days, respectively.

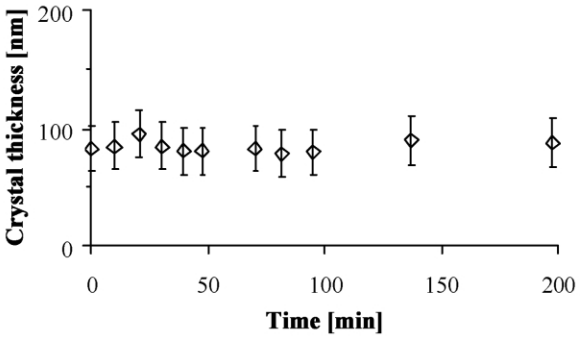

Fig. 7. Crystal thickness versus time data at 69 °C for an individual PEO lamellar crystals. The error bars correspond to the pixel size resolution of these series of images.

crystallinity and assuming a perfect alternating morphology of crystal and amorphous phase.

The estimated values of lamellar thicknesses from the corresponding height images yielded values between two and four times higher as obtained by SAXS, suggesting among other things, the possibility of the presence of lamellar stacks (lamellar crystals). Hence, we cannot make any conclusive statements regarding the dependence of the melting rate on the thickness of the single isolated lamellae based on this data.

Using the series of images consecutively recorded at large time intervals as presented in Fig. 3, we checked the possibility whether isothermal thickening occurred for the high molar mass PEO studied here. The lamellar crystal thickness versus time data is shown in Fig. 7. An average value of 90 nm was estimated for the crystal thickness of one individual lamellar crystal (stack) during the whole isothermal melting experiment. The thickness of the crystal was constant and did not increase in time. This result seems to be contradicting to the low molecular mass PEO crystallization as reported by Kovacs and co-workers [11]. Their LM study revealed that the once folded-chain crystals continued to thicken into extended chain crystals at the temperatures of melting. The lamella increased in thickness by 31.5 nm for the highest molar mass studied (10.000 g/mol). However, it was reported that the isothermal thickening decreased for multi-folded crystals. The results as presented here suggest that the chain diffusion thickening process is unlikely for the multi-folded crystals of high molar mass PEO presumably due to the anchoring of folded polymer chains in the crystals or in the melt.

In Fig. 3 one can note that a reorganization process, consisting of melting of crystals and recrystallization, is absent. This is consistent with the available melting data for PEO as studied by calorimetry as reported by Wunderlich et al. [3,10]. Their studies of melting by standard DSC and temperature modulated differential scanning calorimetry (TMDSC) offered support to the suggestion that there exists only a minor degree of reversible melting in PEO. This minor effect was interpreted as a reorganization process on a molecular or submolecular scale by the authors.

Since our observations are limited to the surface and not to the bulk, the possible influence of surface artifacts should be examined. There are several immediate considerations. The first issue to pursue is the influence of the surface on the kinetics. Several researches have already addressed the possibility of this problem to occur [14,16,17]. On the basis of available growth rate data from LM, they demonstrated that the kinetic data as obtained by AFM were consistent with the overall spherulitic growth rate.

The second issue, that the AFM imaging was performed in air, could be important. A degradation process at the sample–air surface might mislead one to believe that the crystals have melted. Thermogravimetric analysis (TGA) therefore was performed to investigate the thermal stability of PEO. The samples were kept at a temperature of 69 °C under an air atmosphere for 780 min. It was observed that the weight of the sample remained constant during the whole time of annealing/melting. Having thus eliminated oxidative degradation of PEO at the temperatures of observation by AFM, the thermal stability study was extended to an investigation of possible degradation by main chain cleavage. To pursue this matter, the molar mass was measured by GPC of PEO samples before and after melting at 69 °C for 780 min. The peaks in the chromatograms did not shift and thermal degradation by main chain cleavage can be excluded at least for the time scales and temperatures of our AFM melting experiments. Considering the above arguments, it is confirmed that, at least in this particular system, a degradation process at the temperature of the experiments does not obscure the observed processes in PEO.

The third issue is that the crystal initially melts at a constant rate while later in time parts of the crystal seem to 'dissolve' in the melt. The dashed arrows added in the images of Fig. 3(C)–(F) identify the already partially or completely melted crystals and correspond to length data labeled by the open circles and triangles in Fig. 4, respectively. Since the melting process proceeds from the outer side surface of the lamellae to the interior, the observations mentioned seem to result from melting along the z-direction of the images. In principle, the simultaneously recorded height images in Fig. 3 contain information on the melting rates presumably along the (100) direction. The crystals are bounded by {100} faces in the axial direction of the PEO spherulite [12,23]. However, determination of the {100} melting rates failed due to the lack of a fixed reference point with a known height.

To further understand the melting in the z-direction of the AFM images, a method using the indentation depth of the tip has been used. It is well known that the AFM probe experiences a larger indentation in compliant materials [29]. The magnitude of the indentation depends to some extent on the normal load (set-point value). When the set-point value increases the pressure and therefore the indentation depth of the tip also increases. For example, Fig. 8

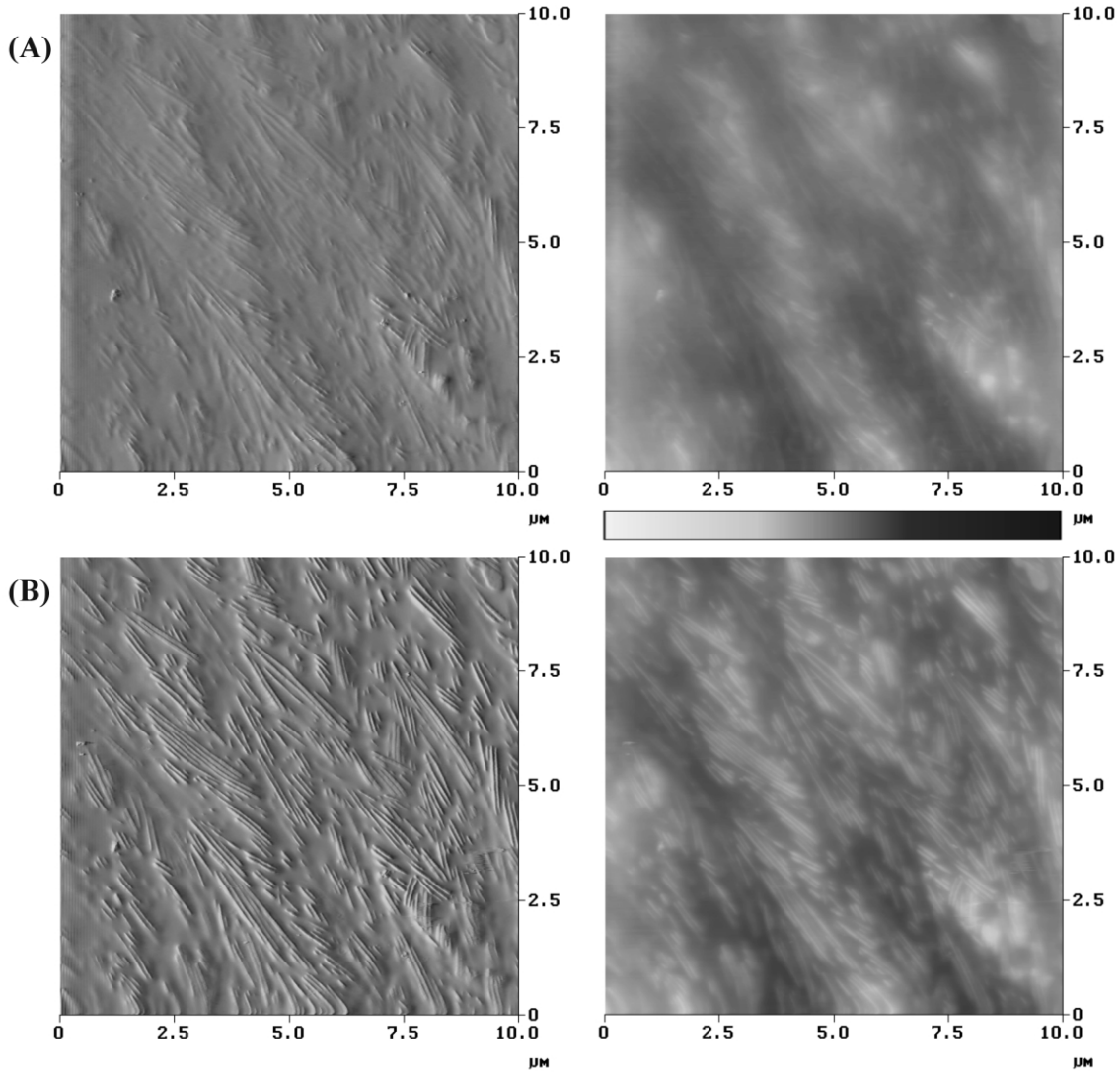

Fig. 8. (A,B) AFM deflection and height images of a PEO spherulite grown at 55 °C for 4 days, obtained at 69 °C. The successive images in (A) and (B) correspond to elapsed times of 193 and 198 min, respectively, with respect to the image in (B) of Fig. 3. The set-point value is increased by 2 V in between capturing the two images. The vertical scale is 500 nm (dark to bright) in both height images.

shows two sets of AFM images obtained at different set-point values. When the set-point value is increased by 2 V in the image of Fig. 8(B) with respect to the imaging conditions used for the images in Figs. 3 and 8(A), the morphology observed changes significantly. The morphology in Fig. 8(B) is similar to the structure observed approximately 100 min earlier (Fig. 3(F)) captured at significantly less load. The deflection image in Fig. 8(A) was obtained after 193 min at 69 °C and shows the continued melting of the PEO crystals into the film. Similar contrast-normal load trends can also be observed in the height images which are recorded simultaneously with the deflection images discussed. It is seen that on increasing the indentation depth of the probe more lamellar crystals appear to be extended above the polymer melt. Using the topography information along similar line scans in the height images, the increase in depth of the probe in the compliant melt phase is estimated to be 10–30 nm. This value is obtained by using the height of the crystals as point of reference, i.e. it is assumed that the increase in indentation depth in the crystal is negligible and that they do not melt significantly in the time required to record the separate images and planar surface.

This latter observation seems wider implacable since it suggests that the protruding of the crystal phase above its melt in contact mode AFM images can be related also to the indentation depth of the tip. Several groups have observed similar protrusion of crystals above the amorphous melt. This effect was observed in AFM morphological studies of PEO [15,17,30] P(HB-*co*-HV) [14,31] polyethylene [22] and poly(bisphenol A octane ether) [20]. The observations are difficult to interpret in view of the volume contraction that occurs during the crystallization process.

The contrast differences between the images in Fig. 8

seem to support that the crystals also melt along the z-direction of the images and therefore appear to 'dissolve' into the melt in time. It should not be taken as contradictory to the results of Pearce et al. where a depletion zone from a three-dimensional contraction of melt was observed at the growth front [14,16,17]. This is a separate process located solely in the soft polymer melt phase.

4. Conclusions

By examining the melting process at a lamellar crystal level, we have established that the melting of the crystals starts either at outer lateral faces or in the interior of the lamellar crystal at presumably defect sites incorporated during the isothermal crystallization. These sites and outer faces are distributed throughout the whole interior of the spherulitic aggregates and explain the different appearance of the melting process as opposed to crystallization when studied by LM.

A general process of melting in terms of a nucleation theory is confirmed. It proceeds by melting of the sections of the polymer chains adsorbed at the outer lateral face. The kinetic data revealed the existence of crystals with different thermodynamic stability. The melting of the PEO crystals seems to be governed by segregation of the polymer chains, which occurs during the growth of the crystals. It is demonstrated that the melting behavior resulting from isothermal crystallization of PEO is not associated with a reorganization process at the melting temperature. Crystal thickening and melting–recrystallization–remelting processes are excluded as contributing factors to the broad melting range as observed for PEO. The broad melting peak as observed in the DSC melting trace is the consequence of the growth of crystals of different lamellar thicknesses at the isothermal crystallization temperature.

In addition, the present study has established the influence of the pressure exerted on the surface by the AFM tips. An interesting characteristic of the AFM contact mode observation is a 'field of depth'. This factor may well contribute to the protruding effect of the crystals observed in the height images.

Acknowledgements

L.G.M. Beekmans would like to thank the Dutch Foundation for Chemical Research (NWO-CW) for a graduate research fellowship and to Prof. S. Muñoz-Guerra (Universitat Politècnica de Catalunya) for helpful discussions. D.W. van der Meer acknowledges the Dutch Polymer Institute (DPI) for financial support.

References

[1] Symposium on Semicrystalline Polymers in memory of Professor Andrew Keller at the ACS National Meeting, New Orleans, August 23–26, 1999. Marand H, Lotz B, editors. Polymer 2000;41:8751–9010.
[2] Bassett DC, Olley RH. Al Raheil IAM. Polymer 1988;29:1745–54.
[3] Cheng SZD, Wunderlich B. J Polym Sci: Polym Phys 1986;24:577–94.
[4] Medellin Rodriguez FJ, Phillips PJ, Lin JS. Macromolecules 1996;29:7491–501.
[5] Ishikiriyama K, Wunderlich B. J Polym Sci: Polym Phys 1997;35:1877–86.
[6] Jaffe M, Wunderlich B. Colloid Polym Sci 1967;216:203–16.
[7] Fischer EW. Pure Appl Chem 1972;31:113–31.
[8] Bassett DC. Phil Trans R Soc Lond A 1994;348:29–43.
[9] Vaughan AS, Bassett DC. Crystallization and morphology. In: Booth C, Price C, editors. Comprehensive polymer science: polymer properties, vol. 2. Oxford: Pergamon Press, 1989. p. 415–57.
[10] Ishikiriyama K, Wunderlich B. Macromolecules 1997;30:4126–31.
[11] Kovacs AJ, Gonthier A, Straupe C. J Polym Sci: Polym Symp 1975;50:283–325.
[12] Kovacs AJ, Gonthier A. J Polym Sci: Polym Symp 1977;59:31–54.
[13] Kovacs AJ, Straupe C. Faraday Discuss Chem Soc 1979;68:225–40.
[14] Hobbs JK, McMaster TJ, Miles MJ, Barham PJ. Polymer 1998;39:2437–46.
[15] Schultz JM, Miles MJ. J Polym Sci: Polym Phys 1998;36:2311–25.
[16] Pearce R, Vancso GJ. Macromolecules 1997;30:5843–8.
[17] Pearce R, Vancso GJ. Polymer 1998;39:1237–42.
[18] Pearce R, Vancso. J Polym Sci: Polym Phys 1998;36:2643–51.
[19] Hobbs JK, Miles MJ. Macromolecules 2001;34:353–5.
[20] Li L, Chan CM, Yeung KL, Li JX, Ng KM, Lei YG. Macromolecules 2001;34:316–25.
[21] Beekmans LGM, Vancso GJ. Polymer 2000;41:8975–81.
[22] Godovsky YK, Magonov SN. Langmuir 2000;16:3549–52.
[23] Marentette JM, Brown GR. Polymer 1998;39:1405–14.
[24] Musevic I, Slak G, Blinc R. Rev Sci Instrum 1996;67:2554–6.
[25] Keith HD, Padden Jr. FJ. J Appl Phys 1963;34:2409–21.
[26] Balta Cellaja FJ, Hay IL, Keller A. Koillod-Z.u.Z. Polymer 1996;209:128–35.
[27] Hoffman JD, Davis GT, Lauritzen Jr. JI. The rate of crystallization of linear polymers with chain folding. In: Hannay NB, editor. Treatise on solid state chemistry, vol. 3. New York: Plenum Press, 1976. p. 497–614.
[28] Cheng SZD, Barley JS, Giusti PA. Polymer 1990;31:845–9.
[29] Burnham NA, Kulik AJ, Gremaud G. Measuring tip–surface interactions. In: Colten RJ, editor. Procedures in scanning probe microscopy, vol. 9. New York: Wiley, 1998. p. 562–84.
[30] Vancso GJ, Beekmans LGM, Pearce R, Trifonova D, Varga J. J Macromol Sci: Phys 1999;B38:491–503.
[31] Kikkawa Y, Inoue Y, Abe H, Iwata T, Doi Y. Polymer 2001;42:2707–10.